Nondielectric long-range solvation of polar liquids in cubic symmetry

Stenhammar, Joakim; Linse, Per; Karlström, Gunnar

Published in:
Journal of Chemical Physics

DOI:
10.1063/1.3250941

2009

Nondielectric long-range solvation of polar liquids in cubic symmetry

Joakim Stenhammar,[1,a)] Per Linse,[1] and Gunnar Karlström[2]
[1]*Division of Physical Chemistry, Center for Chemistry and Chemical Engineering, Lund University, P.O. Box 124, S-221 00 Lund, Sweden*
[2]*Division of Theoretical Chemistry, Center for Chemistry and Chemical Engineering, Lund University, P.O. Box 124, S-221 00 Lund, Sweden*

(Received 4 August 2009; accepted 29 September 2009; published online 28 October 2009)

Long-range solvation properties of strongly coupled dipolar systems simulated using the Ewald and reaction field methods are assessed by using electric fluctuation formulas for a dielectric medium. Some components of the fluctuating electric multipole moments are suppressed, whereas other components are favored as the boundary of the simulation box is approached. An analysis of electrostatic interactions in a periodic cubic system suggests that these structural effects are due to the periodicity embedded in the Ewald method. Furthermore, the results obtained using the reaction field method are very similar to those obtained using the Ewald method, an effect which we attribute to the use of toroidal boundary conditions in the former case. Thus, the long-range solvation properties of polar liquids simulated using either of the two methods are nondielectric in their character. © *2009 American Institute of Physics*. [doi:10.1063/1.3250941]

I. INTRODUCTION

Coulombic and dipole-dipole interactions play important roles in most molecular systems. One preferred method of studying the various effects of these interactions is the use of computer simulations such as Monte Carlo and molecular dynamics (MD) simulations. However, the long-range nature of the electrostatic potentials (r^{-1} and r^{-3}, respectively) makes it crucial to handle the energy calculations of the simulations with great care.

The standard way of avoiding surface effects in molecular simulation is the use of so-called toroidal boundary conditions,[1] often also referred to as periodic boundary conditions. The easiest way of handling the electrostatic interactions in toroidal systems is to simply apply a spherical truncation to the electrostatic potential, thus ignoring the long-range part of the interaction. Although this method seems appealing from a computational perspective, it has been shown to create more or less serious artifacts, depending on the cutoff distance and various other technical details of the cutoff scheme.[2] Another closely related approach is the minimum image (MI) convention, where one employs a cubic cutoff together with toroidal boundary conditions, implying that each molecule interacts with all other particles of the simulation box. Although this approach has been shown to eliminate some of the artifacts of the ST method,[3] the neglect of the long-range nature of the potentials in the MI convention still makes it inadequate for studying strongly electrostatically coupled systems.[4–6]

Among the methods that take into account the infinite range of the electrostatic potential, the lattice summation method originally developed by Ewald[7] in 1921 is probably the most widespread. The basic idea behind the Ewald summation is to include the long-range part of the electrostatic interaction through an infinite cubic lattice of replicas of the central simulation box. Thus, one respects the long-range character of the interactions, albeit while imposing a long-range ordering of the system. Furthermore, using a rigorous analysis of conditionally convergent lattice sums, de Leeuw *et al.*[8] showed that the addition of a surface term U_{surf} given by

$$U_{\text{surf}} = \frac{2\pi}{(2\varepsilon_{\text{RF}}+1)V}\mathbf{M}^2, \tag{1}$$

where $\mathbf{M}$ is the total dipole moment of the simulation box and V its volume, to the electrostatic energy of the system corresponds to embedding the "supersystem" of simulation cells in a dielectric medium with a dielectric constant ε_{RF}. The two common choices of ε_{RF} are $\varepsilon_{\text{RF}}=1$, usually referred to as vacuum boundary conditions, and $\varepsilon_{\text{RF}}=\infty$, referred to as tin-foil boundary conditions. Some highly optimized computational schemes, such as the $\mathcal{O}(N \log N)$ particle-particle particle-mesh Ewald[9] and $\mathcal{O}(N)$ fast multipole[10] methods, have been developed, although these still retain the basic assumption of long-range periodicity of the original Ewald scheme.

An alternative approach for taking into account the long-range part of the electrostatic interactions is the reaction field (RF) method due to Barker and Watts.[11] Within this scheme, the pairwise interactions are subject to a spherical truncation beyond a cutoff radius R_c, whereas the molecules outside the cutoff radius are represented by a dielectric continuum with the dielectric constant ε_{RF} yielding an Onsager-like reaction field $\mathbf{E}_R$ on the molecular system given by[12]

$$\mathbf{E}_R = \frac{2(\varepsilon_{\text{RF}}-1)}{(2\varepsilon_{\text{RF}}+1)R_c^3}\mathbf{M}_S, \tag{2}$$

where $\mathbf{M}_S$ is the total dipole moment of the cutoff sphere. The simplicity of the RF method, together with the avoid-

a)Electronic mail: joakim.stenhammar@fkem1.lu.se.

ance of any long-range periodicity of the system, makes it an appealing alternative to the Ewald summation and related methods. One drawback, however, is the need of knowing, at least approximately, the dielectric constant ε_{RF} of the system before the simulation.

The different computational schemes for treating electrostatic interactions in dipolar systems have been reviewed and evaluated several times before, focusing on different structural and thermodynamic properties.[6,13–16] In the present work, we will use formulas describing the electric fluctuations in dielectric media derived in a recent paper[17] to assess the long-range solvation properties of strongly polar liquids simulated using the Ewald and RF methods, and try to shed some more light on the effects of system periodicity on these properties.

II. THEORY

A. Electric fluctuations in dielectric media

In a previous paper,[17] we derived expressions describing the electric multipole moment fluctuations in a dielectric medium. One of the main results was that the probability distribution $P(Q_{\ell 0})$ of the axial component of a spherical 2^ℓ-pole moment of a spherical volume $Q_{\ell 0}$ (M_ℓ in our previous notation) in a dielectric medium is described by the Gaussian function

$$P(Q_{\ell 0}) = \tilde{a} e^{-\tilde{\alpha} Q_{\ell 0}^2}, \tag{3}$$

with the exponent $\tilde{\alpha}$ given by

$$\tilde{\alpha} = \frac{(2\ell+1)^2 \varepsilon}{2(\varepsilon-1)\ell[(\ell+1)\varepsilon+\ell]} \frac{1}{R^{2\ell+1} kT}, \tag{4}$$

with R representing the radius of the dielectric sphere, ε the dielectric constant of the medium, k the Boltzmann constant, T the absolute temperature, and the spherical multipole moment $Q_{\ell m}$ defined by

$$Q_{\ell m} \equiv \int_V d\mathbf{r} \rho(\mathbf{r}) r^\ell C_{\ell m}(\Omega). \tag{5}$$

In Eq. (5), $\rho(\mathbf{r})$ represents the volume charge density at $\mathbf{r}$ and $C_{\ell m}(\Omega)$ Racah's unnormalized spherical harmonics. The derivation given in Ref. 17 can be extended to nonaxial components of the spherical multipole moments, i.e., $Q_{\ell m}$, $m \neq 0$, in a fully equivalent manner, yielding

$$\langle [\mathrm{Re}(Q_{\ell m})]^2 \rangle = \langle [\mathrm{Im}(Q_{\ell m})]^2 \rangle = \frac{1}{2} \langle Q_{\ell 0}^2 \rangle, \quad m \neq 0, \tag{6}$$

where we have used the mean-square quantities, related with the exponent $\tilde{\alpha}$ through the relationship

$$\langle Q_{\ell 0}^2 \rangle = (2\tilde{\alpha})^{-1}. \tag{7}$$

Furthermore, the solvation free energy A_{solv} related with the interaction of a fluctuating 2^ℓ-pole moment with the surrounding dielectric continuum is given by[17]

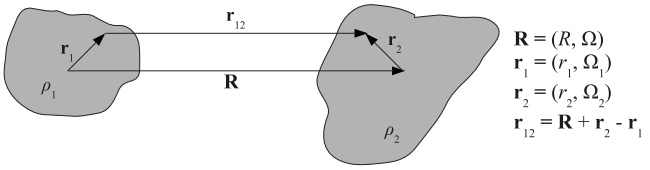

FIG. 1. Illustration of two nonoverlapping charge distributions ρ_1 and ρ_2.

$$\frac{A_{\mathrm{solv}}}{kT} = -\frac{\ell(\ell+1)(\varepsilon-1)^2}{2(2\ell+1)^2\varepsilon}. \tag{8}$$

Equation (8) is valid for both axial and nonaxial components of $Q_{\ell m}$ and reduces to a value of $A_{\mathrm{solv}}/kT \approx \varepsilon/8$ for strongly dielectric systems.

B. Electrostatic self-interactions in a primitive cubic lattice

In this section, we will derive an expression describing the interaction between the spherical multipole moment $Q_{\ell m}$ and its replicas in an infinite primitive cubic lattice. We will henceforth refer to this interaction energy as the *self-interaction* or *self-energy* of $Q_{\ell m}$.

For a given value of ℓ, the spherical multipole moment $Q_{\ell m}$ possesses $2\ell+1$ independent components, namely,

$$Q_{\ell m}^R \equiv \mathrm{Re}(Q_{\ell m}), \quad m = 0, 1, \ldots, \ell, \tag{9a}$$

$$Q_{\ell m}^I \equiv \mathrm{Im}(Q_{\ell m}), \quad m = 1, 2, \ldots, \ell. \tag{9b}$$

In Eq. (9), we have arbitrarily chosen the components with $m \geq 0$ as the independent ones, as the components with $m < 0$ are related with these through the symmetry relation

$$Q_{\ell -m} = (-1)^m Q_{\ell m}^*, \tag{10}$$

where * denotes complex conjugation.

Generally, the electrostatic interaction energy U_{el} between two nonoverlapping charge distributions ρ_1 and ρ_2 is given by[18]

$$U_{\mathrm{el}} = \sum_{\ell_1=0}^{\infty} \sum_{\ell_2=0}^{\infty} \sum_{m_1=-\ell_1}^{\ell_1} \sum_{m_2=-\ell_2}^{\ell_2} \hat{f}(\ell_1, \ell_2, m_1, m_2) \times Q_{1,\ell_1 m_1} Q_{2,\ell_2 m_2} \frac{1}{R^{L+1}} C_{LM}^*(\Omega), \tag{11}$$

where $Q_{i,\ell_i m_i}$ denotes the multipole moment of ρ_i about its origin, R and Ω are defined in Fig. 1, $L = \ell_1 + \ell_2$, and $M = m_1 + m_2$. Furthermore, we have defined the function $\hat{f}$ according to

$$\hat{f}(\ell_1, \ell_2, m_1, m_2) \equiv (-1)^{\ell_1 + M} \left[\frac{(2L)!}{(2\ell_1)!\,(2\ell_2)!} \right]^{1/2} \times \sqrt{2L+1} \begin{pmatrix} \ell_1 & \ell_2 & L \\ m_1 & m_2 & -M \end{pmatrix}, \tag{12}$$

with $(\cdots)$ representing the Wigner $3j$ symbol.

We now consider the electrostatic self-energy $\tilde{U}_{\ell m}^{\mathrm{self}}$ between a central multipole $Q_{\ell m}$ in an infinite primitive cubic lattice and all of its correlated replicas.[19] According to Eqs.

(10) and (11) and using the fact that $\hat{f}(\ell,\ell,m,m)=\hat{f}(\ell,\ell,-m,-m)$, the self-interaction of the different components can be written as

$$\tilde{U}_{\ell 0}^{\mathrm{self},R}=\hat{f}(\ell,\ell,0,0)(Q_{\ell 0}^{R})^{2}\tilde{R}_{2\ell,0}^{*}, \tag{13a}$$

$$\tilde{U}_{\ell m}^{\mathrm{self},R}=2\hat{f}(\ell,\ell,m,m)(Q_{\ell m}^{R})^{2}\tilde{R}_{2\ell,2m}^{*}+2(-1)^{m}\hat{f}(\ell,\ell,m,-m)(Q_{\ell m}^{R})^{2}\tilde{R}_{2\ell,0}^{*},\quad m>0, \tag{13b}$$

$$\tilde{U}_{\ell m}^{\mathrm{self},I}=2\hat{f}(\ell,\ell,m,m)(Q_{\ell m}^{I})^{2}\tilde{R}_{2\ell,2m}^{*}+2(-1)^{m+1}\hat{f}(\ell,\ell,m,-m)(Q_{\ell m}^{I})^{2}\tilde{R}_{2\ell,0}^{*},\quad m>0, \tag{13c}$$

where we have defined the effective interaction tensor $\tilde{R}_{LM}$ according to

$$\tilde{R}_{LM}=\sum_{\mathbf{n}\neq\mathbf{0}}\frac{C_{LM}(\Omega)}{|s\mathbf{n}|^{L+1}}. \tag{14}$$

In Eq. (14), $\mathbf{n}=(n_x,n_y,n_z)$ defines the indices of the unit cells of the primitive cubic lattice, and s denotes the side length of the unit cell. It can be shown that as a consequence of the primitive cubic symmetry, $\tilde{R}_{LM}$ is (i) real and (ii) nonzero only for $L=4+2n$, $n=0,1,2,\ldots$, and $M=0,\pm 4,\ldots,\pm L$. This means that for a given $\ell<4$, the $2\ell+1$ components of $Q_{\ell m}$ for a given ℓ are energetically decoupled from each other. Another consequence of these properties of $\tilde{R}_{LM}$ is that the total dipole-dipole interaction in an infinite primitive cubic lattice is zero. Henceforth, we will refer to the $2\ell+1$ independent components of $Q_{\ell m}$ as *fluctuation modes*.

III. MODEL AND METHODS

A. Model

For the simulation studies, we consider a model system composed of N particles in a cubic volume V at a temperature T. The potential energy U of the system is assumed to be pairwise additive according to

$$U=\sum_{i=1}^{N-1}\sum_{j=i+1}^{N}u_{ij}(r_{ij}). \tag{15}$$

The interaction between molecules i and j, u_{ij}, is composed of a Lennard-Jones (LJ) and a dipole-dipole potential (also referred to as a Stockmayer potential) according to

$$u_{ij}(r_{ij})=u_{ij}^{\mathrm{LJ}}(r_{ij})+u_{ij}^{\mathrm{dip}}(r_{ij}), \tag{16}$$

with

$$u_{ij}^{\mathrm{LJ}}(r_{ij})=4\epsilon\left[\left(\frac{\sigma}{r_{ij}}\right)^{12}-\left(\frac{\sigma}{r_{ij}}\right)^{6}\right], \tag{17}$$

$$u_{ij}^{\mathrm{dip}}(r_{ij})=\frac{1}{4\pi\varepsilon_0}\left[\frac{\boldsymbol{\mu}_i\cdot\boldsymbol{\mu}_j}{r_{ij}^{3}}-\frac{3(\boldsymbol{\mu}_i\cdot\mathbf{r}_{ij})(\boldsymbol{\mu}_j\cdot\mathbf{r}_{ij})}{r_{ij}^{5}}\right], \tag{18}$$

where the size parameter σ and interaction parameter ϵ characterize the LJ interaction, $\boldsymbol{\mu}_i$ denotes the dipole vector of particle i, $\mathbf{r}_{ij}$ is the vector between particles i and j, and $r_{ij}=|\mathbf{r}_{ij}|$.

In this study, we have used the LJ parameters $\sigma=2.8863$ Å and $\epsilon=1.970\,23$ kJ mol^{-1}. The magnitude of the molecular dipole moments equaled $\mu=0.343\,97$ eÅ (corresponding to 0.65 a.u.), and the number density was held fixed at $\rho=0.038\,446$ Å^{-3}. The temperature was kept constant at $T=315.8$ K. In reduced units, the system is characterized by the quantities $\rho^{*}\equiv\rho\sigma^{3}=0.9244$, $T^{*}\equiv kT/\epsilon=1.333$, and $\mu^{*}\equiv\mu/(4\pi\varepsilon_0\epsilon\sigma^{3})^{1/2}=1.863$. Some completing studies using $N=10\,000$ were also performed for particles with dipole moments of $\mu=0.238\,13$ eÅ (0.45 a.u., $\mu^{*}=1.290$) and $\mu=0.105\,84$ eÅ (0.20 a.u., $\mu^{*}=0.5732$) with the same LJ parameters as those described above. The physical parameters of all the systems are identical to those used in Ref. 4.

B. Simulation aspects

The properties of the model systems were determined by performing MD simulations at constant number of particles, volume, and temperature. The particles were enclosed in a cubic box of length a, and periodical boundary conditions were applied. The number of particles N in the system was $N=1000$ ($a=29.629$ Å), $N=10\,000$ ($a=63.833$ Å), $N=100\,000$ ($a=137.52$ Å), and $N=300\,000$ ($a=198.34$ Å), where $N=10\,000$ was used for most of the simulations.

For most of our studies, the long-range dipole-dipole interactions were treated using either (i) the Ewald summation adapted to dipolar systems[7] using conducting as well as vacuum boundary conditions or (ii) the RF method of Barker and Watts.[11] The former approach formally involves an infinite periodic system where the dipole-dipole interaction energy is divided into several terms. For the simulations with $N=10\,000$, an Ewald convergence parameter $\alpha=3.2/R_{\mathrm{cut}}$ was used in conjunction with the spherical cutoff distance $R_{\mathrm{cut}}=19$ Å in real space and the spherical cutoff $n_{\mathrm{cut}}=11$ in reciprocal space. The LJ interactions were subjected to the same spherical cutoff as the dipole-dipole interaction in real space. For the RF simulations, a cutoff equal to half the length of the simulation box was used with the dielectric constant $\varepsilon_{\mathrm{RF}}=130$ of the surrounding dielectric medium.

In addition to the Ewald and RF methods, some simulations were performed using the MI convention.[1] The other parameters describing this system were identical to those used in conjunction with the Ewald and RF methods with $N=10\,000$.

The MD simulations were performed using the velocity Verlet algorithm with the orientations described by quaternions using a time step $\Delta t=0.001$ ps, corresponding to a reduced time step $\Delta t^{*}=\Delta t/(m\sigma^{2}/\epsilon)^{1/2}=0.0011$, where the mass $m=18$ g mol^{-1} was used. The particles were treated as spherical tops with the components of the moment of inertia $I_{xx}=I_{yy}=I_{zz}=1$ g Å^{2} mol^{-1}. Each simulation involved 10^{5} or 10^{6} time steps, hence extending over $t_{\mathrm{sim}}=100$ or 1000 ps. Berendsen's approach[20] of coupling the system to an external bath to preserve the temperature was used with a time coupling constant of $100\Delta t$. This weak coupling only suppresses

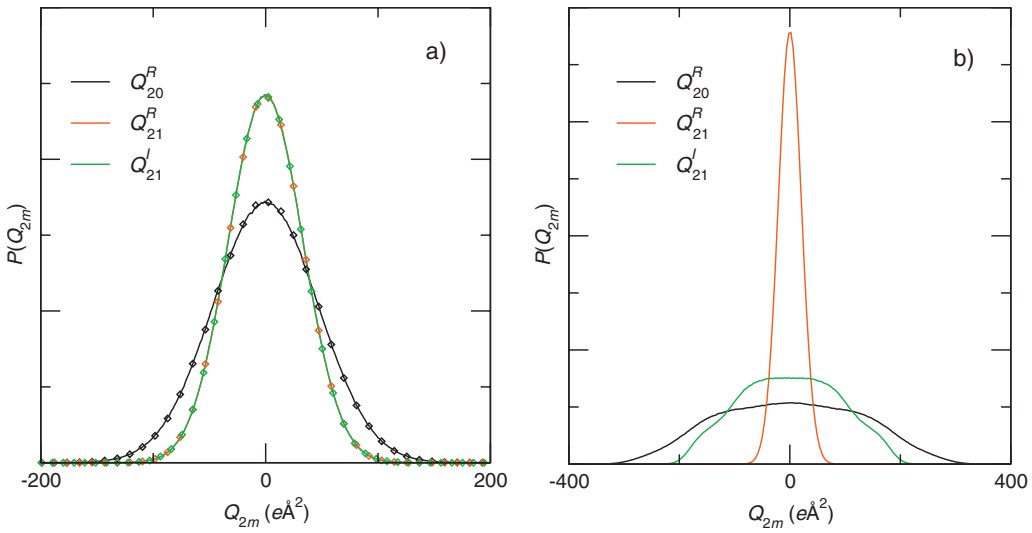

FIG. 2. Probability distributions for three components of the quadrupole moment obtained from simulations using (a) Ewald summation (curves) and the RF method (symbols) and (b) the MI convention using $N=10\,000$ particles and $R=10$ Å.

the potential energy drift and does not affect the dynamics of the system. The integrated Monte Carlo/MD/Brownian dynamics simulation package MOLSIM (Ref. 21) for molecular systems was employed throughout.

C. Fluctuating multipole moment analyses

The magnitude of the fluctuating multipole moments was evaluated after every 100th time step with the contribution from a dipole Q_{1m} located at $\mathbf{R}=(R,\Omega)$ to the moment $Q_{\ell M}$ given by Eq. (A4) in the Appendix. For each evaluated configuration, the values of $Q^X_{\ell m}$ and $(Q^X_{\ell m})^2$, where $X\in\{R,I\}$, $1\leq\ell\leq4$, and $0\leq m\leq\ell$, were sampled for spheres of radii R between 10 Å and $a/2$. Every particle was taken as the origin of a sphere, meaning that for each value of R, N values of $Q^X_{\ell m}$ and $(Q^X_{\ell m})^2$ were sampled per analyzed configuration.

The simulated values $\langle(Q^X_{\ell m})^2\rangle_{\mathrm{sim}}$ were reexpressed as reduced mean-square multipole moments $\Delta^2_{\ell m}$, as defined by

$$\Delta^2_{\ell m}\equiv\frac{\langle(Q^X_{\ell m})^2\rangle_{\mathrm{sim}}}{\langle(Q^X_{\ell m})^2\rangle_{\mathrm{theor}}},\tag{19}$$

where the theoretical values $\langle(Q^X_{\ell m})^2\rangle_{\mathrm{theor}}$ were obtained using Eqs. (4), (6), and (7). Neumann's[22] formula

$$\varepsilon=1+\frac{4\pi}{3}\frac{\langle M^2\rangle}{VkT},\tag{20}$$

relating ε to the mean-square dipole moment $\langle M^2\rangle$ of the entire simulation box for a system treated using Ewald summation with conducting boundaries, was used to obtain the approximate value $\varepsilon=130$ of the system, which was subsequently used for the evaluation of $\langle(Q^X_{\ell m})^2\rangle_{\mathrm{theor}}$.

D. Evaluation of lattice self-interaction energies

Equation (13) was used to numerically evaluate two types of lattice self-energies for $1\leq\ell\leq4$. First, $\tilde{U}^{\mathrm{self}}_{\ell m}$ was calculated using a lattice of unit length, i.e., $s=1$, containing the multipole components $(Q^R_{\ell 0})^2=1$ and $(Q^R_{\ell m})^2=(Q^I_{\ell m})^2=1/2$ for $m>0$, to harmonize with the relative values of Eq. (6). Furthermore, $\langle(Q^X_{\ell m})^2\rangle_{\mathrm{sim}}$, together with putting $s=a$, was used to evaluate the actual self-interaction energies $\langle\tilde{U}^{\mathrm{self}}_{\ell m}\rangle$ of the studied molecular systems. It should be stressed that while $\tilde{U}^{\mathrm{self}}_{\ell m}$ represents an *unweighted* energy where the multipole moment distributions are represented by delta functions, $\langle\tilde{U}^{\mathrm{self}}_{\ell m}\rangle$ represents a *weighted* energy calculated using Boltzmann-weighted distributions of $Q^X_{\ell m}$.

IV. RESULTS AND DISCUSSION

A. Qualitative behavior of probability distributions

Figure 2 shows the probability distributions of three quadrupolar fluctuation modes obtained using the Ewald summation technique, the RF method, and the MI convention. From the Ewald results, it can be seen that the distributions clearly follow the expected Gaussian behavior, something which is also true for the RF results. The distributions obtained using the MI convention are, however, severely distorted compared with the expected appearance, even though the radius of the sampled sphere ($R=10$ Å) is much smaller than the length scale of the simulation box ($a/2=31.9$ Å). Furthermore, it should be noted that by symmetry, the distributions of Q^R_{21} and Q^I_{21} should be identical. This is the case for the Ewald and RF methods, but not for the MI convention, demonstrating that the latter system is nonergodic. Thus, using the MI convention for simulating strongly dipolar systems gives rise to an unphysical behavior of the system. This fact has been established several times before[4–6] and we will therefore not consider the MI results any further.

B. Ewald summation

The values of the reduced mean-squared multipole moment $\Delta^2_{\ell m}$ of various fluctuation modes as a function of the radius R of the sampling volume are given in Figs. 3 and 4 using vacuum and tin-foil boundaries, respectively. From these results, we make the following observations:

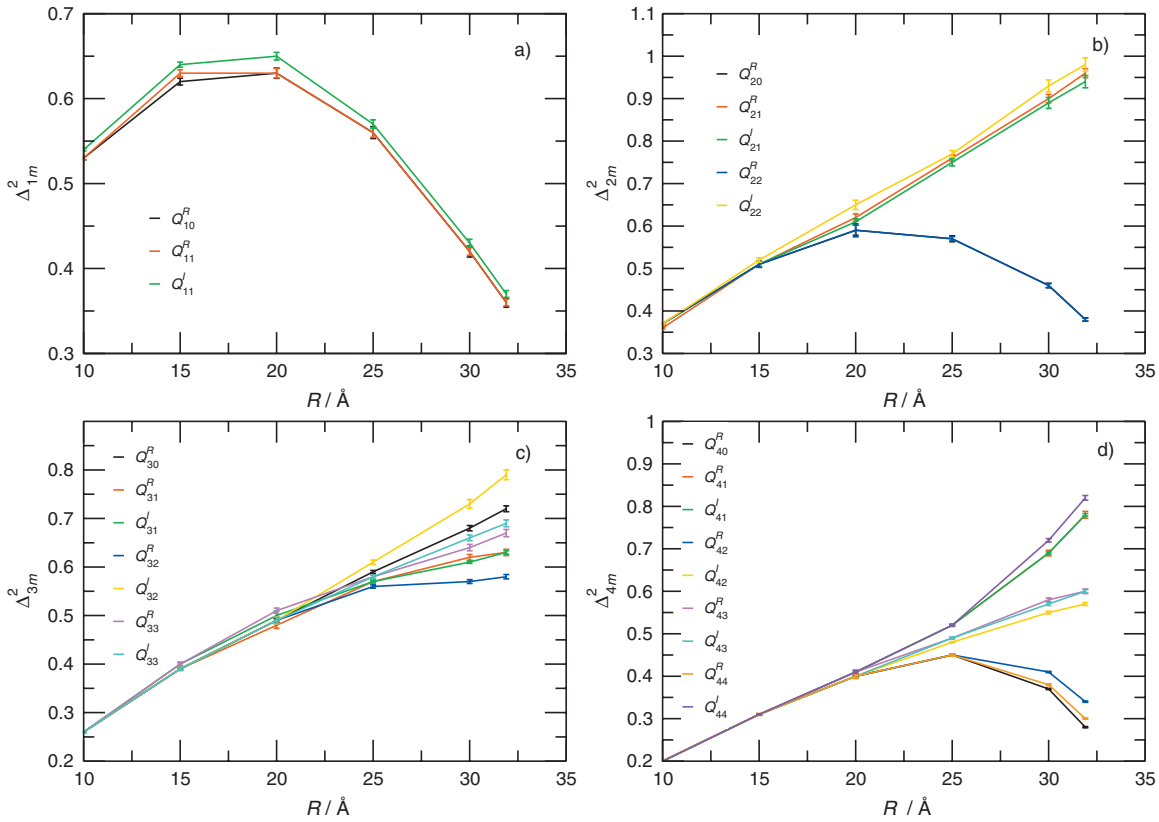

FIG. 3. Reduced mean-squared multipole moment $\Delta^2_{\ell m}$ as a function of the radius R of the sampling volume for $1 \leq \ell \leq 4$ obtained using Ewald summation with vacuum boundaries for a system with $N = 10\,000$ particles. The error bars represent one standard deviation.

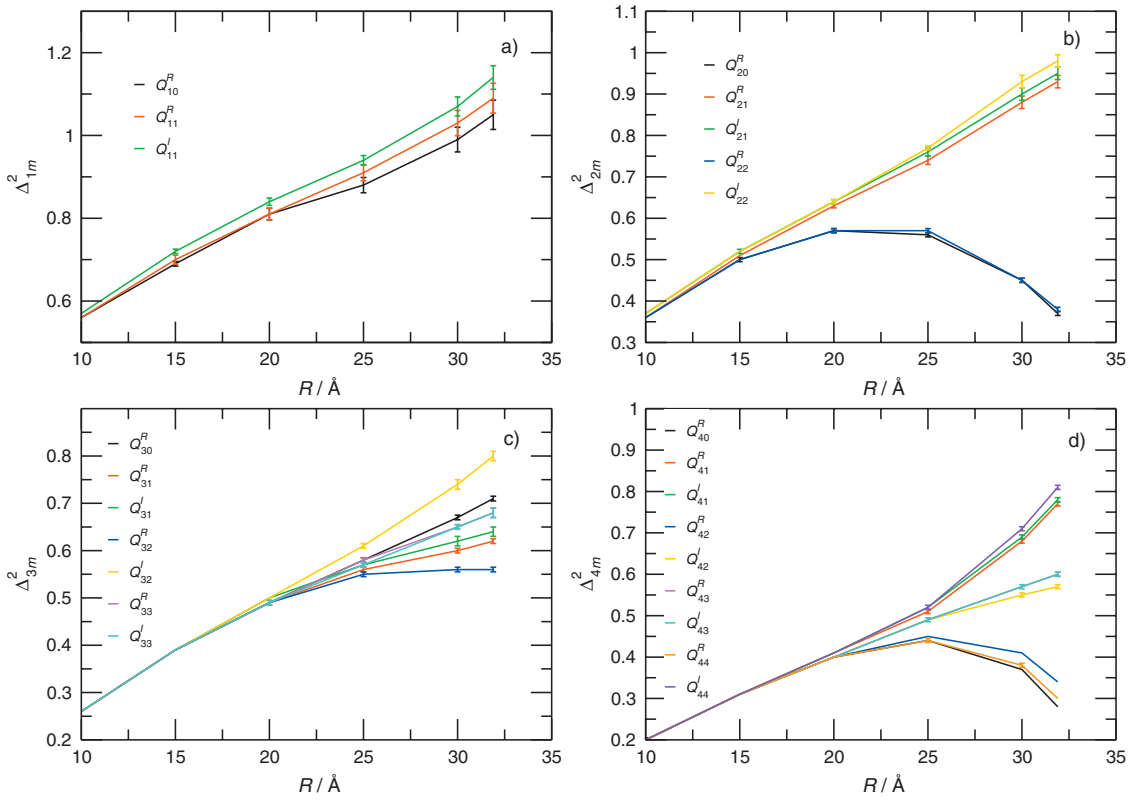

FIG. 4. Reduced mean-squared multipole moment $\Delta^2_{\ell m}$ as a function of the radius R of the sampling volume for $1 \leq \ell \leq 4$ obtained using Ewald summation with tin-foil boundaries for a system with $N = 10\,000$ particles. The error bars represent one standard deviation.

TABLE I. Self-energies of the independent components of the multipole moments $\tilde{U}_{\ell m}^{\mathrm{self}}$ and $\langle \tilde{U}_{\ell m}^{\mathrm{self}} \rangle$ according to Eq. (13). The values used for $Q_{\ell m}$ and s are described in Sec. III D, and the simulated values were obtained from an Ewald simulation with vacuum boundaries and $N=10\,000$.

Mode	$\tilde{U}_{\ell m}^{\mathrm{self}}$ (a.u.)	$\langle \tilde{U}_{\ell m}^{\mathrm{self}} \rangle$ (kJ/mol)
Q_{20}^R	18.6	17.7
Q_{21}^R	−12.4	−29.4
Q_{21}^I	−12.4	−30.0
Q_{22}^R	18.6	17.9
Q_{22}^I	−12.4	−31.2
Sum	**0.0**	**−55.0**
Q_{30}^R	−11.5	−5.3
Q_{31}^R	8.6	3.4
Q_{31}^I	8.6	3.8
Q_{32}^R	20.6	7.6
Q_{32}^I	−27.5	−14.4
Q_{33}^R	0.6	0.2
Q_{33}^I	0.6	0.2
Sum	**0.0**	**−4.7**
Q_{40}^R	228.2	10.6
Q_{41}^R	−182.5	−23.0
Q_{41}^I	−182.5	−23.4
Q_{42}^R	182.5	10.2
Q_{42}^I	0.0	0.0
Q_{43}^R	−26.1	−2.6
Q_{43}^I	−26.1	−2.6
Q_{44}^R	215.1	10.6
Q_{44}^I	−208.6	−27.8
Sum	**0.0**	**−48.0**

(1) For small values of R, all the curves have a positive slope, indicating that the dielectric response is developing gradually.
(2) As the radius of the sampling volume approaches the boundaries of the simulation box, some fluctuation modes are suppressed, whereas others are enhanced.
(3) The effect of the boundaries is more pronounced for even than for odd multipole moments.
(4) Vacuum and tin-foil boundaries give different results for the dipole moment, but within the statistical uncertainties identical results for the higher moments.
(5) The reduced multipole moment fluctuations for $\ell \geq 2$ are in general less than 1, meaning that these moments are not fully developed as compared with the dipole moment in the system simulated using tin-foil boundary conditions, for which the reduced fluctuations are ≈ 1 near the box boundary.

Furthermore, in Table I we give the values of $\tilde{U}_{\ell m}^{\mathrm{self}}$ and $\langle \tilde{U}_{\ell m}^{\mathrm{self}} \rangle$. A comparison between the values of the unweighted quantity $\tilde{U}_{\ell m}^{\mathrm{self}}$ and the curves of Figs. 3 and 4 shows that the order of the curves representing the different fluctuation modes as well as their relative separation follows extremely well the values of $\tilde{U}_{\ell m}^{\mathrm{self}}$. More specifically, the modes that exhibit a net repulsive self-interaction are suppressed, and those interacting attractively are favored near the boundary. This excellent agreement between $\tilde{U}_{\ell m}^{\mathrm{self}}$ and the simulated data indicates that the self-interaction constitutes an important part of the long-range solvation. Looking at the weighted values $\langle \tilde{U}_{\ell m}^{\mathrm{self}} \rangle$, where the simulated values of $\langle (Q_{\ell m}^X)^2 \rangle$ have been used, it is clear that the suppression (enhancement) of the repulsively (attractively) interacting moments is effective, in that the net self-interaction summed over all values of m is considerably attractive, whereas the sum of the unweighted values $\tilde{U}_{\ell m}^{\mathrm{self}}$ is identically zero. Furthermore, we clearly see that the net interaction for $\ell=3$ is an order of magnitude smaller than that for $\ell=2$ and $\ell=4$, in accordance with the comparatively small m-dependence for $\ell=3$ in Figs. 3(c) and 4(c).

An interesting comparison can be made between $\langle \tilde{U}_{\ell m}^{\mathrm{self}} \rangle$ in Table I and the values of A_{solv} as predicted from Eq. (8). Assuming that $\varepsilon=130$ for the studied system, we would expect $A_{\mathrm{solv}} \approx -40$ kJ/mol for each fluctuation mode, which is of the same order of magnitude as the most strongly attractive energies of Table I. In making this comparison, we have neglected the energy contributions coming from other interactions than the self-interaction, i.e., from the interaction between the weakly correlated fluctuation modes, which are included in the theoretical value. Assuming that this is a good approximation, the similarity between $\langle \tilde{U}_{\ell m}^{\mathrm{self}} \rangle$ and the theoretical value of A_{solv} shows that the periodicity of the Ewald method indeed reproduces attractive long-range interactions that are of the same order of magnitude as for a dielectric system, albeit in a different manner. However, as was stated above, the existence of repulsive $\langle \tilde{U}_{\ell m}^{\mathrm{self}} \rangle$ terms still remains as a consequence of the periodicity. It should also be mentioned that the effects described in this section are also observed when simulating significantly less coupled dipolar systems with reduced dipole moments of $\mu^*=1.29$ ($\varepsilon \approx 15$) and 0.57 ($\varepsilon \approx 2.3$). However, the effects are not as strong as for the systems described here.

The system-size dependence of the reduced mean-squared quadrupole moment Δ_{2m}^2 was studied by simulating systems of four different sizes. Figure 5 shows the reduced quadrupole moments as a function of the scaled radius $R/(a/2)$ of the sampling volume. From these results, we make the observations that upon a homogenous size scaling of R and a, (i) the magnitude of Δ_{2m}^2 increases as the length scale of the system is increased, (ii) the onset of the splitting between the different fluctuation modes appears at $R/a \approx 0.25$, regardless of the length scale of the system, and (iii) the splitting in terms of Δ_{2m}^2 is independent of the length scale of the system. Observation (i) indicates that the dielectric coupling is able to become more developed in the larger systems, and hence the dielectric limit has not yet been reached, even for the inner volumes (i.e., for $R \ll a/2$) of the simulation box where the effects from the lattice interactions ought to be small. Observations (ii) and (iii) should be expected, since $U_{\mathrm{el}} \propto Q_{\ell m}^2 R^{-(2\ell+1)}$ according to Eq. (11), and $\langle Q_{\ell m}^2 \rangle \propto R^{2\ell+1}$ according to Eqs. (4) and (7), meaning that the self-interaction of the fluctuation modes should be invariant under size scaling.

Figure 6 displays the same data as in Fig. 5 plus the corresponding data for a system with $N=300\,000$ dipoles as a function of the radius R of the sampling volume with a logarithmic representation on the abscissa. If we now merge

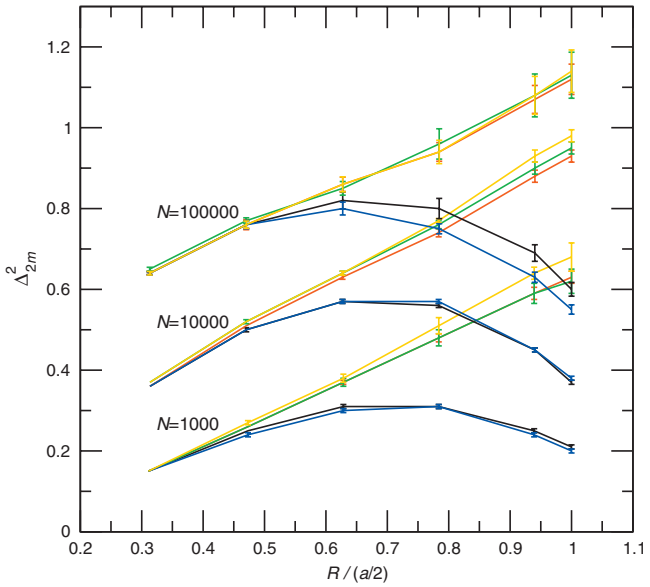

FIG. 5. Reduced mean-squared quadrupole moment Δ^2_{2m} as a function of the reduced radius $R/(a/2)$ of the sampling volume obtained using Ewald summation with tin-foil boundaries at the indicated system sizes. The color labeling is the same as in Fig. 4(b). The error bars represent one standard deviation.

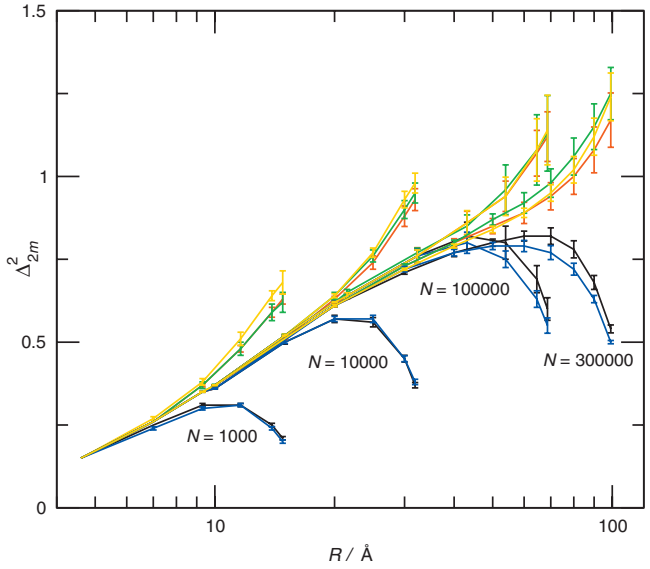

FIG. 6. Reduced mean-squared quadrupole moment Δ^2_{2m} as a function of the radius R of the sampling volume obtained using Ewald summation with tin-foil boundaries at the indicated system sizes. The color labeling is the same as in Fig. 4(b). The error bars represent one standard deviation.

the data for $R/(a/2)<0.25$, which approximately defines the region where no splitting appears, for each system size, we find an essentially linear dependence ranging up to $R\approx 40$ Å. Hence, the reduced mean-squared quadrupole moments depend logarithmically on the radius of the sampling volume up to $\Delta^2_{2m}\approx 0.8$. A corresponding analysis of the dipole moment fluctuations Δ^2_{1m} (not shown here) shows a similar logarithmic dependence in the dielectric behavior of the inner volumes as the system size is increased.

In Table II, we give the values of $\langle \tilde{U}^{\text{self}}_{2,\text{attr}} \rangle$ and $\langle \tilde{U}^{\text{self}}_{2,\text{rep}} \rangle$ for the attractive and repulsive modes of the quadrupole moment for the three different system sizes. The magnitudes of $\langle \tilde{U}^{\text{self}}_{2,\text{attr}} \rangle$ and $\langle \tilde{U}^{\text{self}}_{2,\text{rep}} \rangle$ increase somewhat as the system size is increased, whereas the dielectric behavior as predicted by Eq. (8) implies that they should be invariant under size scaling. From the present data, it is difficult to say anything certain about the convergence of $\langle \tilde{U}^{\text{self}}_{\ell m} \rangle$, although the attractive components seem to approach a limiting value.

C. Reaction field

In Fig. 7, we present the results from the RF simulations. An immediate observation is the striking similarity with the results obtained using the Ewald summation; the behavior of the higher order moments (i.e., with $\ell>1$) is virtually identical to those presented in Figs. 3 and 4. This indicates that the technical details of the RF approach lead to effects that are highly similar to those of the long-range periodicity in the Ewald summation method. One plausible origin of this similarity is the effect stemming from the use of toroidal boundary conditions in the RF method. As depicted in Fig. 8, the fact that each molecule interacts only with the nearest image of the other molecules within the cutoff sphere should give rise to an effective suppression/enhancement of certain multipole moments, in a manner which is highly similar to the periodicity effects in the Ewald method. Although the similarities between the Ewald and RF methods have been somewhat highlighted before,[23] the assumption that the effects arising from periodicity in the Ewald summation technique can be avoided by using the RF method has to be questioned given the near equivalence of the results presented for the two methods.

V. CONCLUSIONS AND OUTLOOK

In the present work, we have presented results that analyze the effect of periodicity and toroidal boundary conditions when simulating strongly dipolar liquids. From the results presented previously,[17] we know that for a dielectric medium, the coupling of higher order moments to the surroundings is energetically at least as important as that of the dipole moment. This implies that it is essential that the long-range solvation properties are correct for all moments, if one intends to simulate a system that behaves as a dielectric medium. However, the results presented here show that this is clearly not the case for a system simulated using the Ewald and RF methods. Indeed, there is a net stabilization of the system arising from the inherent periodicity, as can be seen from the negative net interaction energies in Table I. However, this net solvation is entirely artificial, in the sense that it appears from an imposed periodicity of the system, which is

TABLE II. $\langle \tilde{U}^{\text{self}}_{2,\text{attr}} \rangle$ and $\langle \tilde{U}^{\text{self}}_{2,\text{rep}} \rangle$ calculated from the simulated values of $\langle Q^2_{2m} \rangle$ for systems of three different sizes. The attractive and repulsive values are mean values of the three attractive (Q^R_{21}, Q^I_{21}, and Q^I_{22}) and two repulsive (Q^R_{20} and Q^R_{22}) modes, respectively.

	$N=1000$	$N=10\,000$	$N=100\,000$
$\langle \tilde{U}^{\text{self}}_{2,\text{attr}} \rangle$ (kJ/mol)	−20.3	−30.2	−35.8
$\langle \tilde{U}^{\text{self}}_{2,\text{rep}} \rangle$ (kJ/mol)	9.6	17.8	27.4

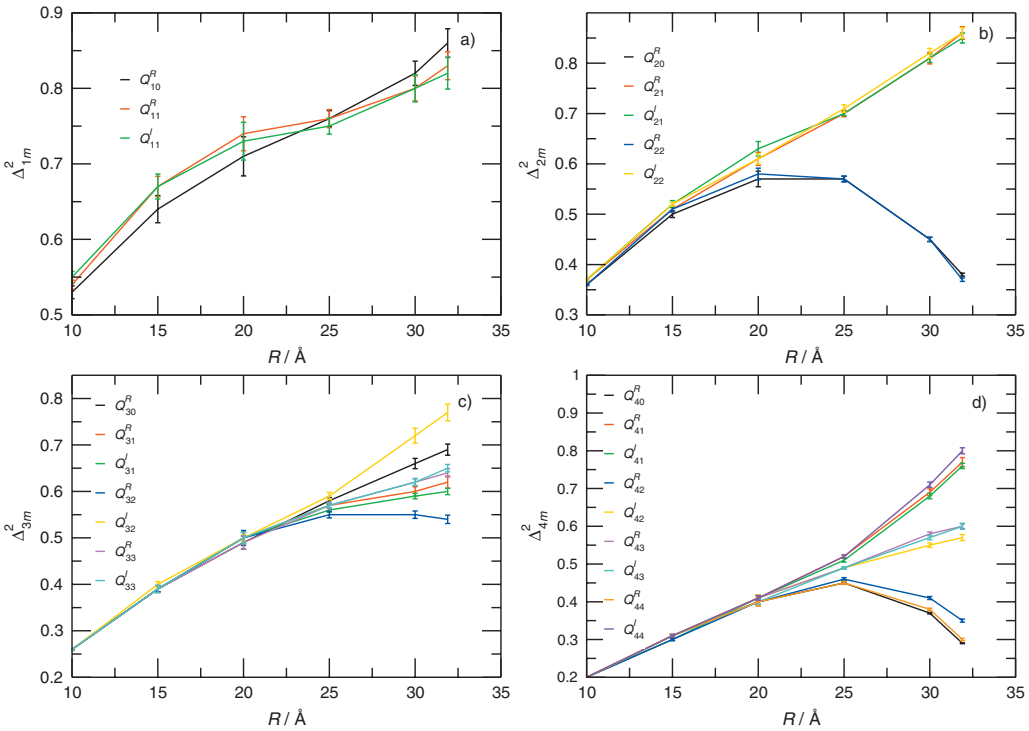

FIG. 7. Reduced multipole moment $\Delta^2_{\ell m}$ as a function of the radius R of the sampling volume for $1 \leq \ell \leq 4$ obtained using the RF approach for a system with $N=10\,000$ particles. The error bars represent one standard deviation.

not present in a real bulk liquid. Furthermore, the solvation energies for several of the fluctuation modes are positive, meaning that these modes are *suppressed* compared with a system in vacuum, an effect which is clearly unphysical.

From the results of Fig. 5, we draw the conclusion that the strong nondielectric effects near the box boundary do not become smaller as the size of the simulated system is increased. However, since the onset of these effects occurs at $R/a \approx 0.25$, regardless of the system size, one possible strategy would be to simulate a system where the inner volumes ($R < 0.25a$) are large enough to exhibit a fully developed dielectric response. Using only the inner volume for the calculation of the dielectric properties of interest should then give reliable results. However, from the results of Fig. 6, we found (i) that $\Delta^2_{\ell m}$ depends logarithmically on the sampling volume up to $\Delta^2_{\ell m} \approx 0.8$ for $\ell = 1$ and 2, and (ii) that the dielectric response is not yet fully developed at a distance of 40 Å. At the present stage it is not possible to judge whether $\Delta^2_{\ell m}$ in general diverges, converges, or converges to unity as predicted by dielectric theory. Regardless of whether there exists a divergence or not, it is obvious that the dielectric response is far from fully developed at 15 Å, which has been reported before from MD simulations of water.[24]

Furthermore, given the limiting behavior ($\ell \to \infty$) of Eq. (8), we do not expect the nondielectric effects to become considerably smaller for moments of higher order than those studied here ($1 \leq \ell \leq 4$), an assumption that gains support from the fact that the effects for the hexadecupole ($\ell = 4$) are essentially as large as those for the quadrupole ($\ell = 2$). Given the strong "selective solvation" effects observed using the above-mentioned techniques, one must ask the question whether these methods are really suitable for calculating dielectric constants and other properties that depend strongly on the long-range coupling in the system. The strong suppression/enhancement of certain moments originates from the creation of an artificial structuring in the system, which should clearly affect its dielectric properties. Some of these effects have been observed before for biomolecules,[25,26] simple charge distributions,[27] and ionic

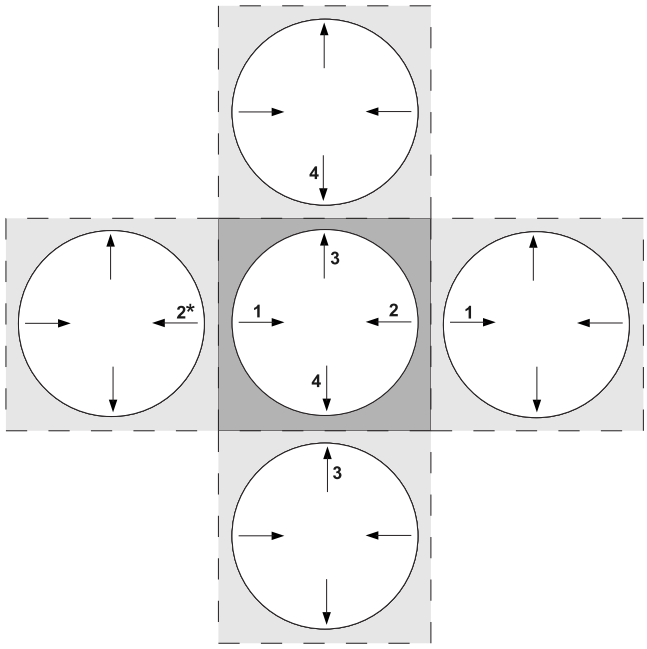

FIG. 8. Illustration of a possible mechanism behind the suppression of fluctuations in the RF method: dipole 1 in the central box interacts repulsively with the nearest image of dipole 2 (labeled with a star), leading to the suppression of the depicted quadrupole moment of the central box. A rotation of the depicted structure by 45° would instead lead to an attractive interaction, which would favor the corresponding fluctuation mode.

systems[28] using the Ewald technique. Furthermore, some general criticism of the periodicity effects present in the Ewald technique was put forward by Valleau and Whittington[29] in the 1970s. However, to our knowledge no similar study has been carried out using the RF technique or using the Ewald technique for dipolar systems.

Since the described periodicity effects are expected to be present in all simulation methods employing toroidal boundary conditions, an interesting question is whether it would be feasible to instead use nonperiodic methods for simulating dielectric systems. This also makes it possible to use simulation cells of any geometry, where spherical geometry is probably the most natural choice. Simulating a spherical cavity, where the molecular system is solvated by a surrounding dielectric medium, would avoid many of the problems described in this paper, albeit while introducing a surface in the system. One possible way to accomplish this is the image charge approach developed by Friedman,[30] where one encloses the particles in a spherical cavity and adds the effect of the surrounding dielectricum through Onsager-like image charges and dipoles. In a forthcoming study, we will assess the usability of this method for studying dielectric properties of systems similar to those that have been described here.

ACKNOWLEDGMENTS

Financial support by the Swedish Research Council (VR) through the Linnaeus grant for the Organizing Molecular Matter (OMM) center of excellence and generous computer time at LUNARC as well as the National Supercomputer Center (NSC) are gratefully acknowledged.

APPENDIX: TRANSLATION OF MULTIPOLE EXPANSION CENTER

We consider the set of multipole moments $Q_{\ell_1 m_1}$ of the charge distribution ρ about the origin according to

$$Q_{\ell_1 m_1} = \int_V d\mathbf{r}_1 \rho(\mathbf{r}_1) r_1^{\ell_1} C_{\ell_1 m_1}(\Omega_1). \tag{A1}$$

The multipole moments of ρ, but with respect to $\mathbf{R}=(R,\Omega)$, are denoted as Q'_{LM} and are given by

$$Q'_{LM} = \int_V d\mathbf{r}_2 \rho'(\mathbf{r}_2) r_2^L C_{LM}(\Omega_2), \tag{A2}$$

where $\mathbf{r}_2=\mathbf{r}_1-\mathbf{R}$. Substitution of $r_2^L C_{LM}(\Omega_2)$ by $|\mathbf{r}_1-\mathbf{R}|^L C_{LM}(\Omega_2)$, and using the expansion of $|\mathbf{r}_1+\mathbf{r}_2|^L C_{LM}(\Omega)$ (Ref. 31), leads to

$$Q'_{LM} = \sum_{\ell_1,\ell_2=0}^{\infty} \sum_{m_1=-\ell_1}^{\ell_1} \sum_{m_2=-\ell_2}^{\ell_2} \hat{f}(\ell_1,\ell_2,m_1,m_2) \times Q_{\ell_1 m_1} R^{\ell_2} C_{\ell_2 m_2}(\Omega), \tag{A3}$$

where we have also made the substitutions $\rho'(\mathbf{r}_2)=\rho(\mathbf{r}_1)$, $d\mathbf{r}_2=d\mathbf{r}_1$, $\ell_1+\ell_2=L$, and $m_1+m_2=M$. In the case when instead Q'_{LM} is placed in the origin and $Q_{\ell_1 m_1}$ at $\mathbf{R}$, we get an extra phase factor $(-1)^{\ell_2}$. Using this, together with restricting ourselves to the special case when $Q_{\ell_1 m_1}=Q_{1m}\delta_{\ell_1 1}$, i.e., a dipole translated from $\mathbf{R}$ to the origin, we obtain after some manipulations

$$Q'_{\ell M} = \sum_{m=-1}^{1} (-1)^{\ell+M} [\ell(2\ell-1)(2\ell+1)]^{1/2} \times \begin{pmatrix} \ell-1 & \ell & 1 \\ M+m & -M & -m \end{pmatrix} Q_{1,-m} R^{\ell-1} C_{\ell-1,M+m}(\Omega). \tag{A4}$$

[1] D. Frenkel and B. Smit, *Understanding Molecular Simulation*, 2nd ed. (Academic, New York, 2002).
[2] P. J. Steinbach and B. R. Brooks, J. Comput. Chem. **15**, 667 (1994).
[3] P. Linse and H. C. Andersen, J. Chem. Phys. **85**, 3027 (1986).
[4] G. Karlström, J. Stenhammar, and P. Linse, J. Phys.: Condens. Matter **20**, 494204 (2008).
[5] D. Levesque, G. N. Patey, and J. J. Weis, Mol. Phys. **34**, 1077 (1977).
[6] D. J. Adams, E. M. Adams, and G. J. Hills, Mol. Phys. **38**, 387 (1979).
[7] P. Ewald, Ann. Phys. **369**, 253 (1921).
[8] S. W. de Leeuw, J. W. Perram, and E. R. Smith, Proc. R. Soc. London, Ser. A **373**, 27 (1980).
[9] R. W. Hockney and J. W. Eastwood, *Computer Simulations Using Particles* (McGraw-Hill, New York, 1981).
[10] A. W. Appel, SIAM (Soc. Ind. Appl. Math.) J. Sci. Stat. Comput. **6**, 85 (1985).
[11] J. A. Barker and R. O. Watts, Mol. Phys. **26**, 789 (1973).
[12] C. J. F. Böttcher, *Theory of Electric Polarization*, 1st ed. (Elsevier, New York, 1952).
[13] D. J. Adams and I. R. McDonald, Mol. Phys. **32**, 931 (1976).
[14] M. Neumann, Mol. Phys. **39**, 437 (1980).
[15] G. Stell, N. Patey, and J. S. Høye, Adv. Chem. Phys. **48**, 183 (1981).
[16] T. M. Nymand and P. Linse, J. Chem. Phys. **112**, 6386 (2000).
[17] J. Stenhammar, P. Linse, P.-Å. Malmqvist, and G. Karlström, J. Chem. Phys. **130**, 124521 (2009).
[18] P. Linse, J. Chem. Phys. **128**, 214505 (2008).
[19] Formally, the requirement that $r_1+r_2<r$ is not fulfilled for all r_1 and r_2 in a cubic lattice. In our further analysis we will, however, limit ourselves to a sphere of radius $a/2$ centered at the origin, thus excluding the corners of the cube where the expansion breaks down from the analysis.
[20] H. J. C. Berendsen, J. P. M. Postma, W. F. van Gunsteren, A. DiNola, and J. R. Haak, J. Chem. Phys. **81**, 3684 (1984).
[21] P. Linse, *MOLSIM* (Lund University, Sweden, 2007).
[22] M. Neumann, Mol. Phys. **50**, 841 (1983).
[23] G. Hummer, L. Pratt, A. Garcia, and M. Neumann, AIP Conf. Proc. **492**, 84 (1999).
[24] G. Mathias and P. Tavan, J. Chem. Phys. **120**, 4393 (2004).
[25] P. H. Hünenberger and J. A. McCammon, Biophys. Chem. **78**, 69 (1999).
[26] M. A. Kastenholz and P. H. Hünenberger, J. Phys. Chem. B **108**, 774 (2004).
[27] P. E. Smith and B. M. Pettitt, J. Chem. Phys. **105**, 4289 (1996).
[28] F. Figueirido, G. S. Del Buono, and L. M. Levy, J. Chem. Phys. **103**, 6133 (1995).
[29] J. P. Valleau and S. G. Whittington, *Statistical Mechanics. Part A: Equilibrium Techniques* (Plenum, New York, 1977), Chap. 4.
[30] H. L. Friedman, Mol. Phys. **29**, 1533 (1975).
[31] D. M. Brink and G. R. Satchler, *Angular Momentum*, 2nd ed. (Clarendon, Oxford, 1968).